



**Repositorio Institucional de la Universidad Autónoma de Madrid**

<https://repositorio.uam.es>

Esta es la **versión de autor** del artículo publicado en:

This is an **author produced version** of a paper published in:

Chemistry - A European Journal 24.46 (2018): 11983-11991

**DOI:** <https://doi.org/10.1002/chem.201801704>

**Copyright:** © 2018 Wiley-VCH Verlag GmbH & Co. KGaA, Weinheim

El acceso a la versión del editor puede requerir la suscripción del recurso

Access to the published version may require subscription

# Impact of Conformational Effects on the Ring-Chain Equilibrium of Hydrogen-bonded Dinucleosides

Carlos Montoro-García,<sup>[a]</sup> Nerea Bilbao,<sup>[a]</sup> Iris M. Tsagri,<sup>[b]</sup> Francesco Zaccaria,<sup>[b]</sup> Maria J. Mayoral,<sup>[a]</sup> Célia Fonseca Guerra<sup>\*[b,c]</sup> and David González-Rodríguez<sup>\*[a,d]</sup>

**Abstract:** Supramolecular ring vs chain equilibria are ubiquitous in biological and synthetic systems. Understanding the factors that decide whether a system will fall into one side or the other is crucial to control molecular self-assembly. Here, we report our results with two kinds of dinucleoside monomers in which the balance between closed cycles and open polymers is found to depend on subtle factors that rule conformational equilibria, such as steric hindrance, intramolecular interactions or  $\pi$ -conjugation pathways.

## Introduction

Supramolecular polymers are formed from molecules with (at least) two complementary sites that bind through noncovalent interactions.<sup>[1-3]</sup> Depending primarily on molecular structure, diverse noncovalent polymerization mechanisms can operate under thermodynamic conditions.<sup>[4]</sup> Among them, ring-chain equilibria,<sup>[5]</sup> where discrete cyclic/closed assemblies compete with linear/open polymers, may be considered as the most fundamental one.<sup>[6,7]</sup>

A key phenomenon ruling these polymerization processes is chelate (or intramolecular) cooperativity, which defines the predisposition of a molecule or an assembly to cyclize.<sup>[8]</sup> It operates in the natural world in protein folding or DNA hybridization processes,<sup>[9]</sup> and in synthetic chemistry in a wide variety of discrete supramolecular architectures: helicates, ladders, grids, macrocycles, cubes, prisms, capsules, etc.<sup>[10-13]</sup> Commonly, adequately preorganized rigid monomers and directional noncovalent interactions, provide high chelate effects, so cycle formation dominates over polymerization at relatively low concentrations. If, on the other hand, cyclization leads to strained structures and/or to a substantial loss of degrees of

conformational freedom, a distribution of linear assemblies will be primarily formed.

Due to its importance in biological and synthetic chemistry, many researchers have investigated diverse noncovalent systems with the aim to unravel the key structural parameters that decide to which side a molecule will fall in these ring (*i.e.* macrocycle)-chain (*i.e.* polymer) equilibria.<sup>[14]</sup> Here, we report our results with two kinds of systems (Figure 1) in which the balance between closed and open systems depends on conformational preferences, which are at the same time defined by subtle structural changes.

During the last few years we have studied the self-assembly of molecules comprising two complementary nucleosides linked through a rigid, linear spacer (Figure 1).<sup>[15]</sup> Such monomers can associate by Watson-Crick H-bonding interactions and establish a ring-chain equilibrium in solution. The  $\sigma$ -bonds in the spacer allow the nucleobases to rotate and alternate between two main planar conformations in which these aromatic heterocycles and the central blocks maintain  $\pi$ -conjugation through the ethynylene spacers. We specifically call them *syn* and *anti* conformations, depending if the Watson-Crick edges are arranged, respectively, at the same or opposite sides (see Figure 1a). Participation of the *anti* conformation results in the formation of supramolecular polymers, whereas the exclusive involvement of the *syn* conformation leads to cyclotetramerization. We previously demonstrated that **GC1** cyclic tetramers (**cGC1<sub>4</sub>**) are formed quantitatively in solvents of moderate polarity due to the strong chelate effects attained.<sup>[15a]</sup> More recent work in our group focused on evaluating the dependence of the length of the phenylene-ethynylene spacer connecting the two bases (*n* in Figure 1b) on chelate cooperativity.<sup>[15c]</sup> Different monomers were prepared in which *n* varied from 1 to 5. A thorough thermodynamic study revealed that cycle stability decreased substantially as the monomer length increased. This trend had a clear entropic origin, related to the degrees of freedom that are lost upon cyclization, and was proportional to the number of  $\sigma$ -bonds in the spacer, which are the main responsible for rotational and torsional motions and thus for giving access to multiple conformations.

These previous results would then induce to think that either 1) reducing further the number of  $\sigma$ -bonds in the spacer or 2) blocking the rotational/torsional freedom of one or more of these  $\sigma$ -bonds, would enhance chelate effects and lead to higher cyclization yields. These two situations are analyzed herein independently. We discovered that making such changes in the monomer structure, however, actually brings steric and electronic effects that have a strong impact in ruling *syn-anti* conformational preferences and thus on deciding to which side, ring or chain assemblies, the system will fall.

[a] Dr. C. Montoro-García, Dr. N. Bilbao, Dr. M. J. Mayoral, Prof. D. González-Rodríguez  
Nanostructured Molecular Systems and Materials group, Organic Chemistry Department, Universidad Autónoma de Madrid, 28049 Madrid, Spain  
E-mail: [david.gonzalez.rodriguez@uam.es](mailto:david.gonzalez.rodriguez@uam.es)

[b] Iris M. Tsagri, F. Zaccaria, Prof. C. Fonseca Guerra  
Theoretical Chemistry and ACMM, Vrije Universiteit Amsterdam, The Netherlands  
E-mail: [c.fonseca Guerra@vu.nl](mailto:c.fonseca Guerra@vu.nl)

[c] Prof. C. Fonseca Guerra  
Leiden Institute of Chemistry, Gorlaeus Laboratories, Leiden University, The Netherlands

[d] Prof. D. González-Rodríguez  
Institute for Advanced Research in Chemical Sciences (IAdChem), Universidad Autónoma de Madrid, 28049 Madrid Spain

Supporting information for this article is given via a link at the end of the document.

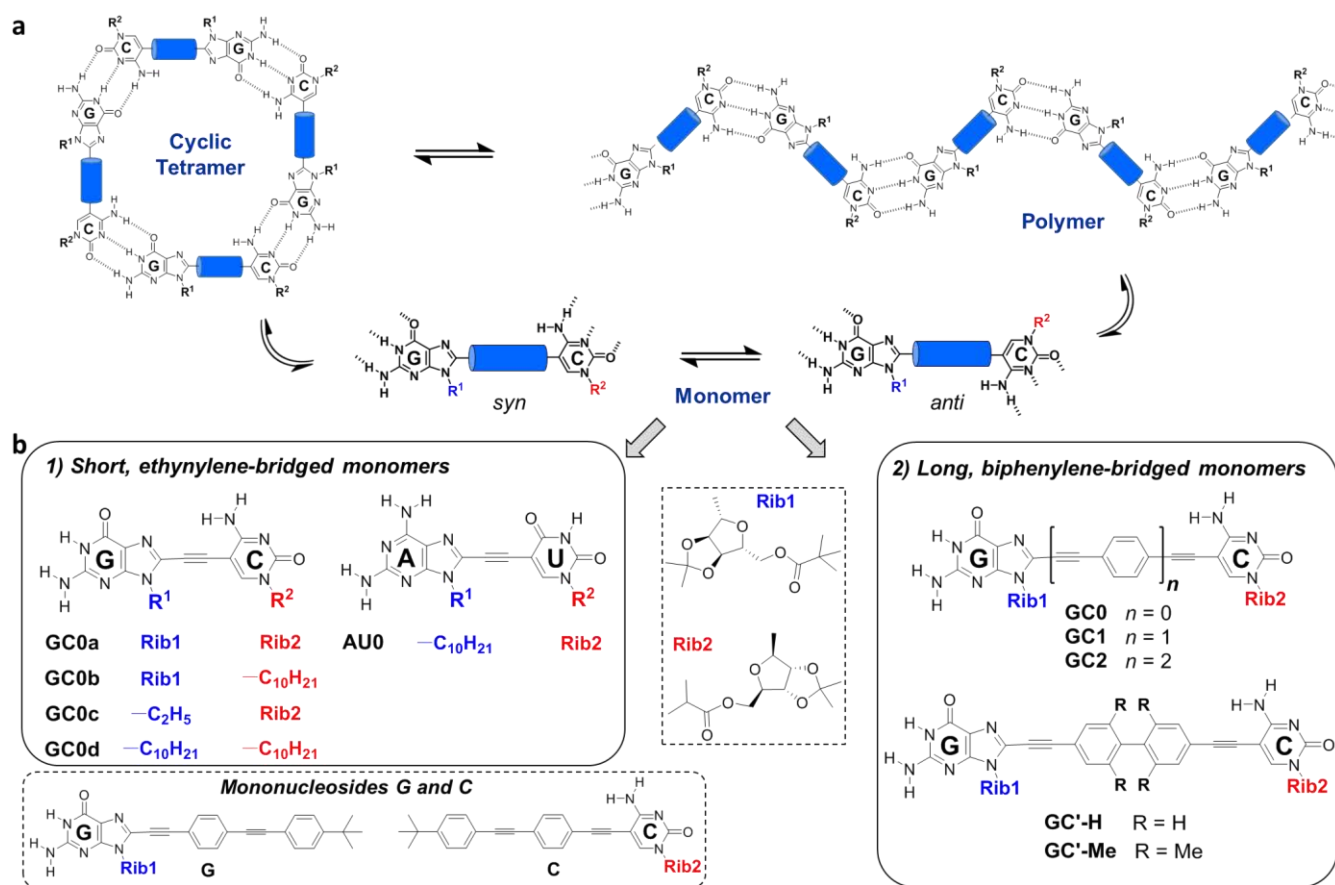


**Figure 1.** a) Ring-chain equilibrium established by G-C dinucleoside monomers. b) Ethynylene- (GC0a, AU0), ethynylene-phenylene- (GC1, GC2) and biphenylene-bridged (GC'-H, GC'-Me) monomers. Please note that 2-aminoadenine (or 2,6-diaminopurine) is abbreviated here as **A** for the sake of simplicity, and should not be confused with adenine.

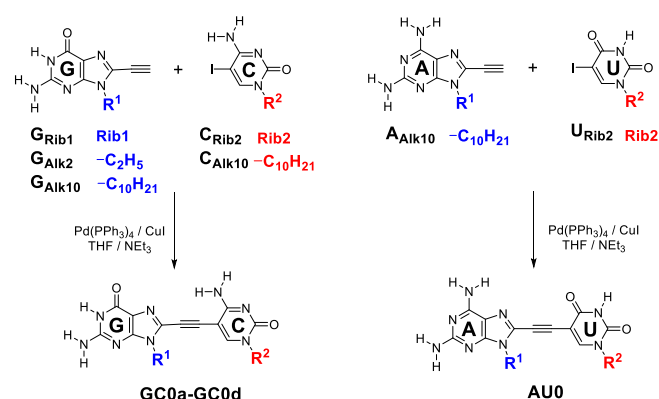
## Results and Discussion

### 1) Short, ethynylene-bridged dinucleoside monomers.

To evaluate the impact of a reduced number of  $\sigma$ -bonds in the spacer, 5 novel ethynylene-linked molecules (Figure 1b) were synthesized and studied both experimentally in solution and with computational DFT methods. One of these monomers contain the 2-aminoadenine (abbreviated here as **A**)-uracil (**U**) pair (**AU0**) and four of them the guanine (**G**)-cytosine (**C**) pair (**GC0a-d**), and differ in the substituents placed at the purine *N*-9 and at the pyrimidine *N*-1. All these novel molecules were prepared by Pd-catalyzed Sonogashira cross-coupling reactions between 8-ethynyl-purines (**G**<sub>Rib1</sub>, **G**<sub>Alk2</sub>, **G**<sub>Alk10</sub> or **A**<sub>Alk10</sub>; see Scheme1) and the corresponding 5-iodo-pyrimidines (**C**<sub>Rib2</sub>, **C**<sub>Alk10</sub> or **U**<sub>Rib2</sub>), as detailed in the experimental section. On the other hand, these ethynylated or halogenated nucleobase precursors were synthesized following previously published methods.<sup>[16,17]</sup>

We reasoned that reducing the distance between nucleobases might also bring new effects that were not dominant or absent in the larger monomers (*i.e.*  $n = 1-5$ ). On one hand, steric effects between the bulky lipophilic riboses would be higher in the *syn* conformation, the one required for cyclization. Moreover, intramolecular interactions between the groups in the heterocycle and/or the substituents may also arise. Additionally, as the length of the  $\pi$ -conjugated linker becomes shorter, electronic

(anti)cooperative effects might arise in highly apolar solvents in which binding of one Watson-Crick edge may electronically affect binding strength at the opposite edge.<sup>[18]</sup>



With the aim of maintaining the same ribose substitution pattern as in our previous work,<sup>[15]</sup> **GC0a** was first synthesized. We soon found out that **GC0a** is either insoluble ( $\text{CH}_3\text{OH}$ ,  $\text{CH}_3\text{CN}$ ,

acetone, diethyl ether, cyclohexane, and heptane) or forms strong gels after heating and cooling back to room temperature in a variety of solvents (toluene, benzonitrile, THF,  $\text{CHCl}_3$ ,  $\text{CHCl}_2\text{CHCl}_2$  and chlorobenzene). The microstructure of these gels examined by SEM (Figures 2a-b) revealed characteristic fibers that are connected and entangled all over the surface.<sup>[19]</sup> This behaviour strongly contrasts the one shown by longer monomers (**GC1**, **GC2**) of identical ribose substitution pattern, which always afforded clear non-viscous solutions.<sup>[15]</sup>

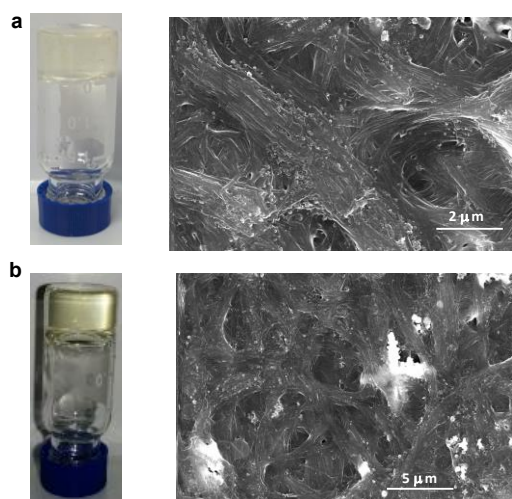


**Figure 2.** Inverted vial pictures and SEM images of **GC0a** in (a) chlorobenzene and (b) benzonitrile.

This anomalous self-assembly behaviour seemed to indicate that the *anti* conformation in **GC0a** could be heavily populated due to the influence of intramolecular interactions and/or steric effects between the bulky ribose substituents (*vide infra*). Therefore, we decided to prepare 3 additional G-C monomers (**GC0b-d**) in which steric hindrance was released by substituting one or both of the bulky riboses by linear alkyl chains. Their supramolecular behaviour, falling either into the formation of polymers or cycles, was already evident from their solubility and gelation ability. Whereas **GC0b** exhibited similar characteristics as **GC0a**, forming gels in a variety of solvents, **GC0c** and **GC0d**, although not extraordinarily soluble, were unable to gelate any solvent.

NMR analysis of the different samples further confirmed the self-assembly differences of **GC0a/b** and **GC0c/d**. Although a wide variety of experiments as a function of temperature or concentration in diverse solvents ( $\text{CDCl}_3$ , THF- $\text{D}_8$ ,  $\text{CDCl}_2\text{CDCl}_2$ ) were executed, not all conditions provided well-resolved  $^1\text{H}$  signals due to the scarce solubility of these short dinucleosides, which hampered quantitative analysis.<sup>[15]</sup> The most informative experiment was the change in solvent polarity by gradually increasing DMSO- $\text{D}_6$  content in  $\text{CDCl}_3$ -DMSO- $\text{D}_6$  mixtures at constant concentration, as shown in Figure 3 for four different samples: 1) a 1:1 mixture of **G** and **C** mononucleosides (see Figure 1b for molecular structure), 2) **GC0a**, 3) **GC0c**, and 4) a longer, previously studied monomer (**GC1**) where  $n = 1$ .<sup>[15a]</sup>

In the 1:1 mixture of **G** and **C** mononucleosides, the shape and position of the G amide and C amine  $^1\text{H}$  NMR probes change significantly when increasing the DMSO- $\text{D}_6$  content, suggesting fast equilibria in the NMR timescale between the **G:C** complex and **G** and **C** solvated molecules. This situation strongly contrasts

the behaviour of our reference **GC1** dinucleoside,<sup>[15]</sup> where a slow exchange is noted between the solvated monomer (10.8 ppm; marked in red) and G:C H-bonded cyclic tetramer (**cGC1<sub>4</sub>**) signals (13.4 and 10.0 ppm; marked as red and blue squares). As the macrocycle is progressively dissociated in the presence of this H-bonding-competing cosolvent, the solvent-bound G-amide proton in the monomeric **GC** species grows at the expense of the original **cGC<sub>4</sub>** signals. Now, when analysing **GC0a-b** in the same way, we found extremely broad  $^1\text{H}$  NMR spectra at low DMSO content, suggesting the formation of large aggregates. As the solvent polarity increases, the degree of H-bonding is diminished and the monomer, detected by the G-amide signal at 10.8 ppm, is released into solution. An inspection of the NMR tube reveals that gelation is disrupted and viscosity is reduced upon addition of DMSO- $\text{D}_6$  along these titrations. On the contrary, **GC0c-d**, substituted by linear alkyl groups at the purine heterocycle, offered again two main sets of signals in slow exchange at low DMSO contents, that then disappear to yield the monomer signal at higher polarities. This behaviour is reminiscent of **GC1**, and indicates that **cGC0c<sub>4</sub>** and **cGC0d<sub>4</sub>** are also formed in  $\text{CDCl}_3$  solutions, although the  $^1\text{H}$  NMR spectra are, unfortunately, not that well-resolved. If we attend to the amount of DMSO required to dissociate the macrocycles, the following stability trend is found: **cGC1<sub>4</sub>** >> **cGC0d<sub>4</sub>** > **cGC0c<sub>4</sub>**, which indicates a lower cycle stability for the shorter monomers. Unfortunately a CD analysis like we did in previous work<sup>[15]</sup> could not be performed here with the aim to obtain quantitative data since all these short monomers without central phenylene rings are CD-inactive.

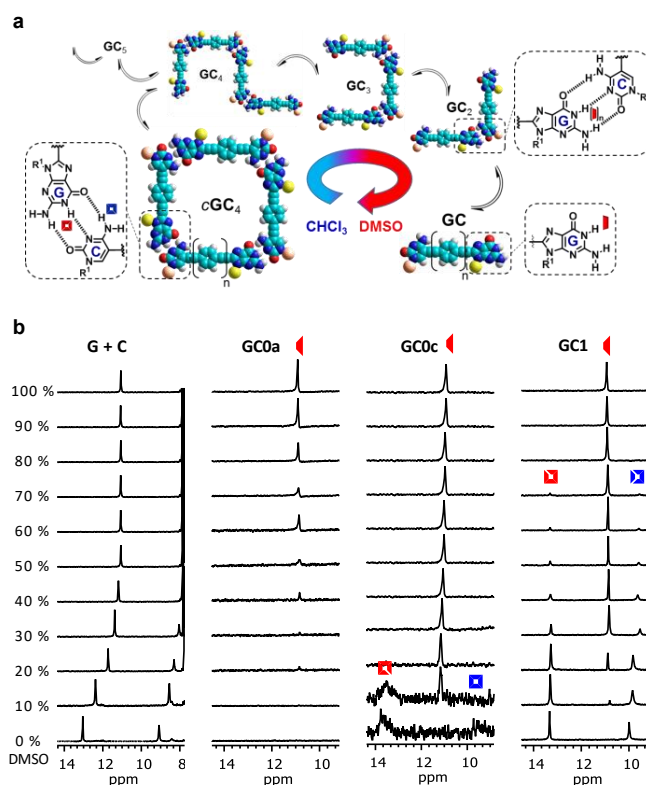


**Figure 3.** a) General scheme showing the disassembly of a cyclic tetramer as the DMSO content is increased in  $\text{CHCl}_3$ . b) Downfield region of the  $^1\text{H}$  NMR spectra, showing the H-bonded G-H amide (red) and C-H amine (blue) signals of a 1:1 **G+C** mononucleoside mixture (see Figure 1b), **GC0a**, **GC0c**, and **GC1** as the volume fraction of DMSO- $\text{D}_6$  is increased in  $\text{CDCl}_3$ -DMSO- $\text{D}_6$  mixtures at  $C = 1.0 \times 10^{-2}$  M and  $T = 298$  K.

On the other hand, when examining the behaviour of a related monomer with A-U bases (**AU0**; Figure S1) no trace of the **cAU0<sub>4</sub>** cycle was obtained and the results indicated the presence of weakly interacting short oligomers. This behaviour was somehow expected, in view of the lower association constant and chelate effects afforded by the A:U interaction.<sup>[15b]</sup>

In order to shed light on the irregular supramolecular behaviour of these shortly spaced monomers, we performed calculations using the Amsterdam Density Functional (ADF) program and dispersion-corrected density functional theory at the BLYP-D3(BJ)/DZP, for geometry optimization, and BLYP-D3(BJ)/TZ2P, for energies. Solvation in CHCl<sub>3</sub> was simulated using the conductor-like screening model (COSMO).<sup>[20]</sup>

For **GC0a**, the *anti* conformer is 3.0 kcal/mol more stable than the *syn*, while for **GC0b**, **GC0c** and **GC0d**, the computations showed that *syn* and *anti* conformations are equally stable (-0.5, -0.2 and -0.3 kcal/mol difference, respectively). The steric clash in **GC0a-b** was then investigated by substituting the nucleobases by H atoms (see Figure 4a) and computing the interaction between the side-chains. The computations revealed that there is no repulsion, but actually a slight attraction between side chains of -3.8 kcal/mol (**GC0a**) and -2.4 kcal/mol (**GC0b**) in the gas phase (see S.I.). This is merely a consequence of the subtle balance between steric repulsion and attractive interactions, such as dispersion and electrostatic interactions (Table S1). In other words, the substituents at the nucleobases are able to find conformations in which steric effects are absent in the *syn* planar arrangement, even in the most heavily crowded **GC0a** (see Figure 4a). On the other hand, computations on the **GC0** and **GC1** cyclic tetramers with R<sup>1</sup>=R<sup>2</sup>=Me showed no electronic cooperativity in the H-bonding energy (Table S2), meaning that the binding of one nucleobase does not affect electronically to the binding of the adjacent one through the covalent,  $\pi$ -conjugated spacer.<sup>[18a]</sup>

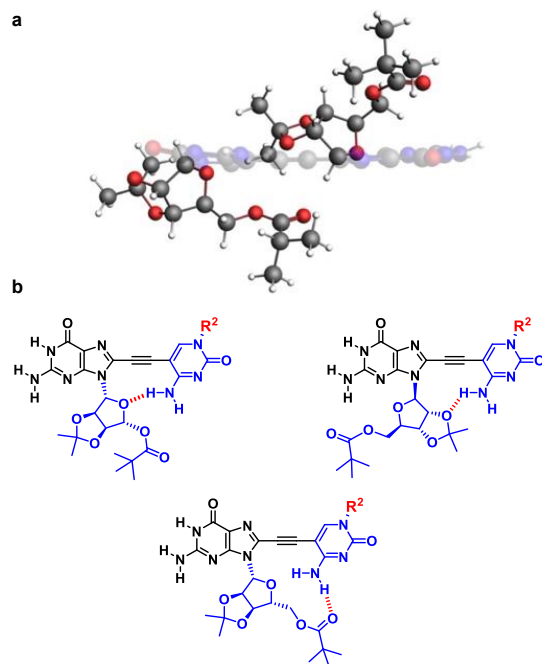


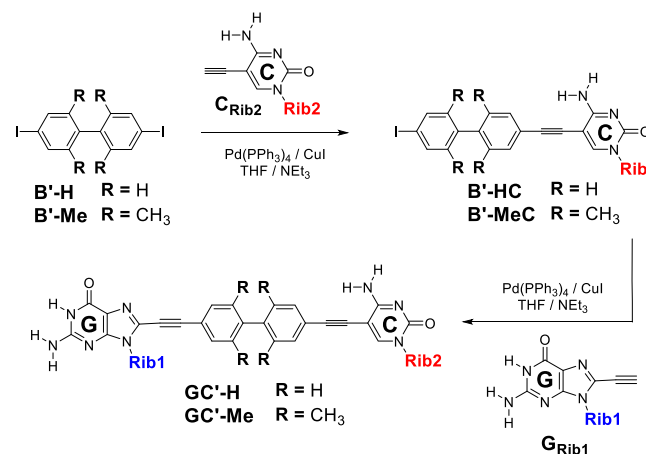
**Figure 4.** a) Rib1 and Rib2 groups (highlighted) and nucleobases G and C (faded) for **GC0a** in a *syn* conformation. b) Possible intramolecular H-bonds patterns in **GC0a/GC0b** that can stabilize the *anti* conformer.

These findings led us to think that a reason different from steric hindrance or electronic effects might be responsible for the stability of the *anti* conformer in **GC0a-b**. An inspection of their structures revealed the existence of diverse possible H-bonding interactions between the C-amino group and the different oxygen atoms in the G-ribose moiety (from left to right in Figure 4b): the cyclic ether's, the dioxolanic or the pivalic carbonyl oxygens. The H-bonds computed for the most stable species amount to -4.5 and -3.9 kcal/mol, respectively, for **GC0a** (H-bonded to the cyclic ether's oxygen) and **GC0b** (to the dioxolane oxygen) in the gas phase; they were computed by elimination of the G heterocycle and the linker (black atoms in Figure 4b). The species in which the H-bond involves the pivalic carbonyl oxygen are, on the contrary, less favourable (~10 kcal/mol) than the *syn* conformer of **GC0a-b**.

In short, the combination of our experimental and theoretical results leads to the conclusion that the possibility of formation of different intramolecular H-bonds between the C-amino group and the ether groups at the G-ribose moiety of **GC0a** and **GC0b** in the *anti* conformation is very likely to determine a substantial hindrance to their mutual rotation, blocking the structures in a spatial configuration that is unfavourable for cyclization and making the formation of linear polymers highly predominant.

## 2) Long, biphenylene-bridged dinucleoside monomers.

Our next case study consists in monomers equipped with biphenylene central blocks (**GC'-H** and **GC'-Me**; see Figure 1b and the experimental section for synthetic details). In contrast to the phenylene-ethynylene spacers in **GC1-GC2**, having Csp-Csp<sup>2</sup> aryl-ethynyl  $\sigma$ -bonds, the biphenyl moieties cannot adopt perfectly planar conformations and rotation around the central Csp<sup>2</sup>-Csp<sup>2</sup> bond is sterically hindered to a small extent (**GC'-H**) or totally blocked (**GC'-Me**).<sup>[21]</sup> The synthesis of these two new dinucleoside compounds (Scheme 2) follows a similar route to the one exploited by us before.<sup>7</sup> It comprises two subsequent standard Sonogashira couplings on the corresponding 4,4'-diodobiphenyl derivatives (**B'-H** and **B'-Me**), first with **C<sub>Rib2</sub>**, to yield **B'-HC** and **B'-MeC**, and then with **G<sub>Rib1</sub>** to afford the final dinucleoside monomers.



**Scheme 2.** Synthesis of ethynylene-bridged G-C monomers **GC0a-d** and A-U monomer **AU0**.



Figure 5 shows  $^1\text{H}$  NMR experiments in which we monitor again aggregate dissociation by gradually increasing the DMSO- $\text{D}_6$  content in  $\text{CDCl}_3$ . Let's first compare **GC'-H**, having 5  $\sigma$ -bonds, one of them a  $\text{Csp}^2\text{-Csp}^2$  bond, with **GC1** and **GC2**, having 4 or 6  $\text{Csp-Csp}^2$   $\sigma$ -bonds, respectively. All these dinucleosides show qualitatively the same behavior: an all-or-none monomer-cyclic tetramer equilibrium where these two species are in slow exchange in the  $^1\text{H}$  NMR timescale, without significant participation of other open oligomers. Their relative stability can be estimated by comparing the amount of DMSO that is needed for full macrocycle dissociation. The trend obtained is rather clear: **cGC1**<sub>4</sub> > **cGC2**<sub>4</sub> > **GC'-H**<sub>4</sub>. That is, even if the number of  $\sigma$ -bonds is lower in **GC'-H** when compared to **GC2**, its relative stability is clearly lower.

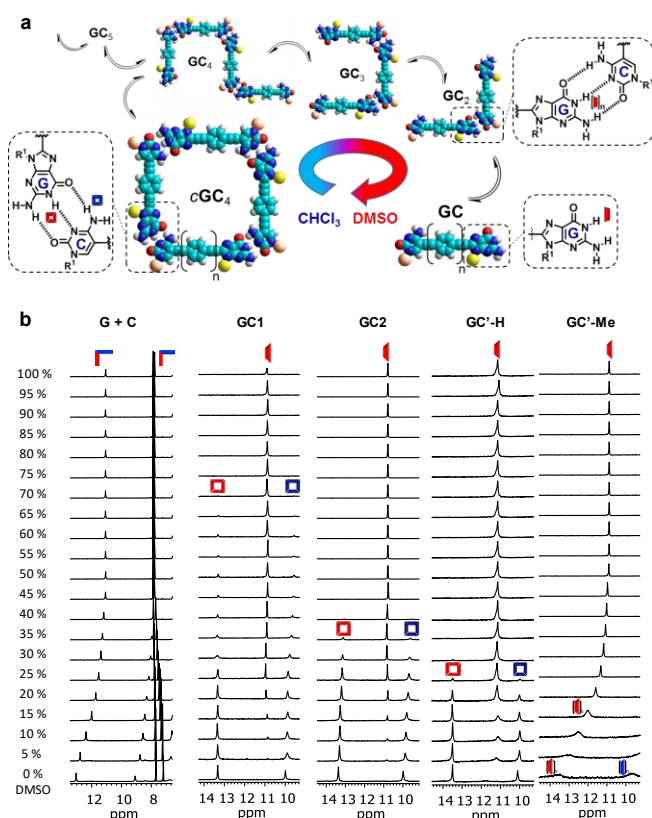


**Figure 5.** a) General scheme showing the disassembly of a cyclic tetramer as the DMSO content is increased in  $\text{CHCl}_3$ . b) Downfield region of the  $^1\text{H}$  NMR spectra of a 1:1 **G+C** mixture and of **GC1**, **GC'-H**, **GC2** and **GC'-Me** dinucleosides as the volume fraction of DMSO- $\text{D}_6$  is increased in  $\text{CDCl}_3$ -DMSO- $\text{D}_6$  mixtures at  $C = 1.0 \cdot 10^{-2}$  M and  $T = 298$  K.

When moving to **GC'-Me** we observed again a radical change in the self-assembly picture that is more consistent with polymerization than with the formation of discrete assemblies. In particular: 1)  $^1\text{H}$  NMR and DOSY experiments in  $\text{CDCl}_3$  revealed very broad signals characteristic of a distribution of H-bonded oligomers; 2) adding DMSO- $\text{D}_6$  or diluting this monomer in polar solvents such as THF- $\text{D}_8$  or DMF- $\text{D}_7$  resulted in a gradual upfield shift of the H-bonded proton signals, very similar to the one monitored for the 1:1 **G+C** mixture (Figure 5b), which sharply contrasts the kinetic stability and the all-or-nothing features observed for the other monomers that can form cycles; and 3)

**GC'-Me** afforded viscous solutions or gels in apolar solvents like  $\text{CHCl}_3$ ,  $\text{CHCl}_2\text{CHCl}_2$ , THF or toluene.

The stability of the **GC'-H** cyclic tetramers was also evaluated and compared through denaturation experiments in which increasing amounts of a **C** nucleoside stopper were gradually added to **GC1**, **GC2** or **GC'-H** solutions in  $\text{CDCl}_3$  (Figure 6). In these measurements, the mononucleoside competes with the dinucleoside for binding to the complementary base, and the titration with **C** progressively transforms the **cGC4** tetramolecular macrocycle into a **C·GC** bimolecular complex (Figure 6a). We found that this is a very useful method to directly evaluate the chelate cooperativity of a cyclic system, since both reactants and products are Watson-Crick G-C-bound species and the outcome only depends on the molecularity and the cyclic/non-cyclic nature of the assemblies present in solution at the beginning and at the end of the titration.<sup>[15a]</sup> Since **cGC4** is a kinetically stabilized species in the NMR timescale, both **cGC4** and **C·GC** afford separate signals in slow exchange, whereas the excess of **C** mononucleoside in solution is in fast exchange with **C·GC**.

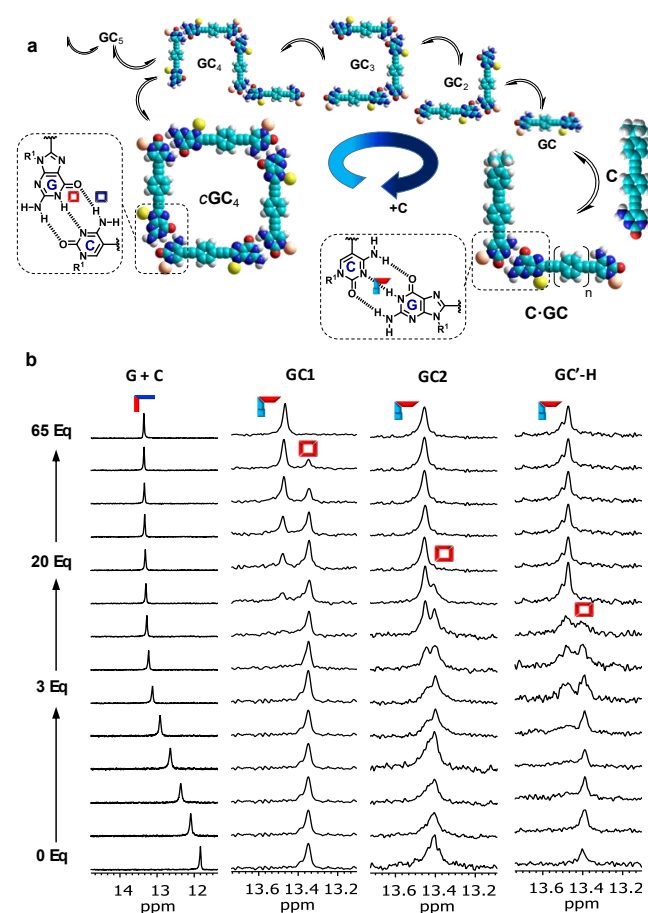


**Figure 6.** a) Scheme showing the disassembly of a cyclic tetramer as increasing amounts of **C** mononucleoside (see Figure 1b for chemical structure) are added. b) Changes observed in the G-amide region of the  $^1\text{H}$  NMR spectra of **G** and of **GC1**, **GC2** and **GC'-H** ( $C = 1.0 \cdot 10^{-2}$  M,  $\text{CDCl}_3$ ,  $T = 298$  K) by adding increasing amounts of **C**.

As can be observed in Figure 6b, as higher amounts of **C** are added, a new G-amide proton signal, corresponding to the H-bonded **C·GC** complex, arises at slightly downfield chemical shifts

(ca. 13.5 ppm) and increases in intensity at the expense of the original **cGC**<sub>4</sub> signals. The G-C binding interaction is the same in both **cGC**<sub>4</sub> and **C·GC** assemblies, as well as for all rings. However, the amount of competing mononucleoside that is needed to observe the total disappearance of the **cGC**<sub>4</sub> <sup>1</sup>H NMR signals is very different and considerably decreases in the same order as that observed for the addition of DMSO: **GC1** > **GC2** > **GC'-H**.

In short, the formation of cyclic species is slightly (**GC'-H**) or totally (**GC'-Me**) inhibited as steric hindrance around the biphenyl *Csp*<sup>2</sup>-*Csp*<sup>2</sup> bond increases and this group is forced to orient the phenyl groups in orthogonal planes (blue and red planes in Figure 7).<sup>[21a]</sup> Still, a cyclic tetramer could be formed if the monomer is able to adopt a conformation in which the nucleobases are in the same plane (as *I* or *III*). These conformers would allow  $\pi$ -conjugation through the ethynylene spacers by maintaining the pyrimidine (*I*) or the purine (*III*) heterocycle in a 90° angle with respect to the adjacent phenyl ring. However, our experimental observations provided no evidence for **cGC'-Me**<sub>4</sub> macrocycle formation. This seems to indicate that the **GC'-Me**  $\pi$ -conjugated system (and to a lower extent, **GC'-H**) might prefer to adopt conformation *II*, where each nucleobase is conjugated to the adjacent phenyl ring in the same plane through the ethynylene group, thus leaving the two nucleobases in orthogonal planes. This monomer geometry makes the formation of a cycle impossible and the only option left for **GC'-Me** is to polymerize.

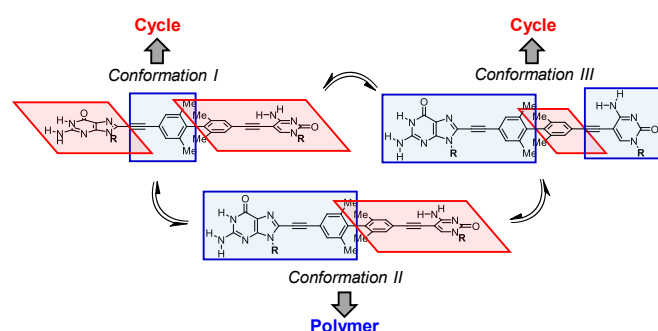


**Figure 7.** Possible  $\pi$ -conjugated conformations adopted by **GC'-Me**, obtained by 90° rotation around the *Csp*-*Csp*<sup>2</sup>  $\sigma$ -bonds. Blue and red planes are orthogonal to each other. Conformations *I* and *III* maintain the two bases in the same plane, and might thus lead to the formation of cyclic tetramers. However, in conformation *II* the two bases are in orthogonal planes and Watson-Crick pairing should only lead to open supramolecular polymers.

In order to confirm this hypothesis, we again performed calculations, as described above, using simplified models of **GC'-Me**, where the riboses were substituted by methyl groups. The three conformations were in turn optimized leading to full relaxation (no constraints applied) and constraining 4 dihedral angles in order to fix the relative characteristic plane orientations between the bases and the spacers (Table S3). According to these computations, conformation *II* is indeed 1.3 kcal/mol more stable than conformation *I* and 0.9 kcal/mol more stable than conformation *III* (based on constrained models). From full geometry optimizations, while conformation *II* is still 0.8 kcal/mol more stable than conformation *III*, conformation *I* doesn't appear to be represented, since it autonomously switches to conformer *II*.

## Conclusions

The novel dinucleoside monomers prepared and studied in this work represent a direct proof of how delicate can be the balance between ring formation and supramolecular polymerization. A supramolecular system may fall on one side or the other not only depending on molecular geometry and rigidity, but also as a function of diverse factors that rule conformational equilibria, such as steric hindrance, intramolecular interactions or  $\pi$ -conjugation pathways.

## Experimental Section

**General Methods.** LSI-MS and HR-MS spectra were determined on a VG AutoSpec apparatus, ESI-MS spectra were obtained from an Applied Biosystems QSTAR equipment. NMR spectra were recorded with a BRUKER AVANCE-II (300 MHz) instrument and BRUKER DRX 500 MHz. The temperature was actively controlled at 298 K. Chemical shifts are measured in ppm using the signals of the deuterated solvent as the internal standard [CDCl<sub>3</sub> calibrated at 7.26 ppm (<sup>1</sup>H) and 77.0 ppm (<sup>13</sup>C), DMSO-D<sub>6</sub> calibrated at 2.50 ppm (<sup>1</sup>H) and 39.5 ppm (<sup>13</sup>C)]. Column chromatography was carried out on silica gel Merck-60 (230-400 mesh, 60 Å), and TLC on aluminium sheets precoated with silica gel 60 F254 (Merck). SEM images were recorded with a Philips XL30 S-FEG microscope.

**Starting materials.** Chemicals were purchased from commercial suppliers and used without further purification. Solid hygroscopic reagents were dried in a vacuum oven before use. Reaction solvents were thoroughly dried before use using standard methods. The synthesis and characterization of compounds **G1**, **C1**, **U1**,<sup>[16a]</sup> **G1Aik2**, **C1Aik10**, **G1Aik10**, **A1Aik10**,<sup>[16b]</sup> and **GC0d**,<sup>[22]</sup> have been recently reported by us. **B'-Me**<sup>[23]</sup> have been reported elsewhere and their identity was checked only by <sup>1</sup>H NMR. **B'-H** was purchased from commercial suppliers. The synthesis of the different dinucleoside monomers are detailed below (see the S.I. for additional information).

**Synthetic Standard Procedure A for the Sonogashira coupling between the ethynyl-nucleobase and iodoarene.** A dry THF/NEt<sub>3</sub> (4:1) solvent mixture was subjected to deoxygenation by three freeze-pump-thaw cycles with argon. Then, this solvent was added over the system containing the corresponding ethynyl-substituted base (1 eq.), halogenated base (1.2 eq.), CuI (0.01 eq.) and Pd(PPh<sub>3</sub>)<sub>2</sub>Cl<sub>2</sub> (0.02 eq.). The reaction is stirred under argon at a given temperature and for a period of time (indicated in each case) until completion, which was monitored by TLC. Then, the mixture was filtrated over celite and the solvent evaporated under vacuum. The resulting crude product was purified by column chromatography (eluent indicated in each case).

**Synthetic Standard Procedure B for the Sonogashira coupling between the ethynyl-nucleobase and iodoarene.** A dry THF/NEt<sub>3</sub> (4:1) solvent mixture was subjected to deoxygenation by three freeze-pump-thaw cycles with argon. Then, this solvent was added over the system containing the corresponding ethynyl-substituted base (1 eq.), iodoarene (5 eq.), CuI (0.01 eq.) and Pd(PPh<sub>3</sub>)<sub>2</sub>Cl<sub>2</sub> (0.02 eq.). The reaction is stirred under argon at a given temperature and for a period of time (indicated in each case) until completion, which was monitored by TLC. Then, the mixture was filtrated over celite and the solvent evaporated under vacuum. The resulting crude product was purified by column chromatography (eluent indicated in each case).

**GC0a** was prepared according to a *Standard Procedure A* for the Sonogashira coupling reaction between iodo-nucleobase **C1** and the ethynyl-nucleobase **G1**. A dry a THF/NEt<sub>3</sub> (4:1) mixture (10 mL) was

poured over **G1** (200 mg 0.5 mmol), PdCl<sub>2</sub>(PPh<sub>3</sub>)<sub>2</sub> (6.5 mg, 9.3 μmol), and CuI (0.88 mg, 4.6 μmol). Then, **C1** (289 mg, 0.6 mmol) was added and the mixture was stirred under argon for 12h at 40 °C. Once completed, the mixture was filtrated over a celite plug and the solvent was evaporated under reduced pressure. The product was purified by recrystallization in acetonitrile, affording **GC0a** as a white solid (316 mg, 81 %). <sup>1</sup>H NMR (300 MHz, CDCl<sub>3</sub>: [D<sub>6</sub>]DMSO, 25°C, TMS): δ= 11.00 (s (broad), 1H; NH<sup>16</sup>C), 8.16 (s, 1H; H<sup>6C</sup>), 8.99 (s (broad), 1H; NH<sup>4C</sup>), 7.31 (s (broad), 1H; NH<sup>4C</sup>), 6.80 (s (broad), 2H; NH<sub>2</sub><sup>2G</sup>), 6.15 (s, 1H; H<sup>1G</sup>), 5.85 (s, 1H; H<sup>1C</sup>), 5.47 (d, <sup>3</sup>J(H,H)=6.3 Hz, 1H; H<sup>2C</sup>), 5.30 (dd, <sup>3</sup>J(H,H)=6.2, <sup>4</sup>J(H,H)=4.0 Hz, 1H; H<sup>2C</sup>), 5.02 (dd, <sup>3</sup>J(H,H)=6.4, <sup>3</sup>J(H,H)=1.6 Hz, 1H; H<sup>3G</sup>), 4.87–4.84 (m, 1H; H<sup>3C</sup>), 4.38–4.13 (m, 6H; H<sup>4G</sup>, H<sup>5G</sup>, H<sup>4C</sup>, H<sup>5C</sup>), 2.68–2.58 (m, 1H; COCH), 1.54 (d, <sup>3</sup>J(H,H)=7.9 Hz, 6H; -OC(CH<sub>3</sub>)), 1.35 (d, <sup>3</sup>J(H,H)=9.8 Hz, 6H; -OC(CH<sub>3</sub>)), 1.12 (s, 15H; -COCH-(CH<sub>3</sub>)<sub>2</sub>, -COC(CH<sub>3</sub>)<sub>3</sub>). <sup>13</sup>C NMR (75 MHz, CDCl<sub>3</sub>: [D<sub>6</sub>]DMSO, 25°C, TMS): δ= 179.4, 177.8, 164.6, 159.5, 155.7, 154.4, 150.8, 145.0, 121.8, 118.1, 114.2, 113.4, 95.8, 94.6, 93.2, 92.4, 89.3, 87.7, 85.4, 85.0, 84.2, 83.5, 81.4, 79.4, 79.1, 77.8, 76.5, 76.4, 76.1, 66.3, 64.2, 38.1, 33.2, 29.4, 27.8, 27.6, 27.5, 25.8, 25.6, 19.5. HRMS (FAB+): *m/z* calcd for C<sub>36</sub>H<sub>47</sub>N<sub>8</sub>O<sub>12</sub>: 783.3313 [*M*+*H*]<sup>+</sup>; found: 783.3334 [*M*+*H*]<sup>+</sup>.

**GC0b** was prepared between iodo-nucleobase **C<sub>alk10</sub><sup>[8b]</sup>** and the ethynyl-nucleobase **G1**. A dry a THF/NEt<sub>3</sub> (4:1) mixture (12 mL) was poured over **C<sub>alk10</sub><sup>[8b]</sup>** (100 mg 0.23 mmol), PdCl<sub>2</sub>(PPh<sub>3</sub>)<sub>2</sub> (3.3 mg, 4.6 μmol), and CuI (0.4 mg, 2.3 μmol). Then, **G1** (105 mg, 0.28 mmol), was added and the mixture was stirred under argon for 12h at 40 °C. Once completed, the mixture was filtrated over a celite plug and the solvent was evaporated under reduced pressure. The product was purified by column chromatography on silica gel eluted with CHCl<sub>3</sub>/MeOH (10:1), affording **GC0b** as a white solid (149 mg, 73 %). <sup>1</sup>H NMR (300 MHz, CDCl<sub>3</sub>: [D<sub>6</sub>]DMSO, 25°C, TMS): δ= 10.86 (s (broad), 1H; NH<sup>16</sup>C), 8.19 (s, 1H; H<sup>6C</sup>), 7.48 (s (broad), 1H; NH<sup>4C</sup>), 6.71 (s (broad), 1H; NH<sup>4C</sup>), 6.58 (s (broad), 2H; NH<sub>2</sub><sup>2G</sup>), 6.12 (s, 1H; H<sup>1G</sup>), 5.39 (d, <sup>3</sup>J(H,H)=6.2 Hz, 1H; H<sup>2C</sup>), 5.20 (s, 1H; H<sup>3G</sup>), 4.28–4.03 (m, 3H; H<sup>4G</sup>, H<sup>5G</sup>), 3.72 (t, <sup>3</sup>J(H,H)=7.1 Hz, 2H; -NCH<sub>2</sub>-), 1.50 (s, 3H; -OC(CH<sub>3</sub>)), 1.31 (s, 3H; -OC(CH<sub>3</sub>)), 1.21 (s, 16H; -CH<sub>2</sub>-), 1.09 (s, 9H; -COC(CH<sub>3</sub>)<sub>3</sub>), 0.82 (s, 3H; -CH<sub>3</sub>). <sup>13</sup>C NMR (75 MHz, CDCl<sub>3</sub>: [D<sub>6</sub>]DMSO, 25°C, TMS): δ= 177.6, 164.6, 156.7, 154.6, 154.3, 152.4, 150.7, 129.9, 117.5, 113.7, 88.9, 87.0, 86.3, 85.8, 84.0, 83.8, 82.0, 64.7, 49.7, 38.6, 31.7, 29.4, 29.3, 29.1, 29.1, 29.0, 27.4, 27.2, 26.3, 25.7, 22.5, 14.4, 0.6. HRMS (MALDI; Matrix: DCTB): *m/z* calcd for C<sub>34</sub>H<sub>49</sub>N<sub>8</sub>O<sub>7</sub>: 681.3719 [*M*+*H*]<sup>+</sup>; found: 681.3740 [*M*+*H*]<sup>+</sup>.

**GC0c** was prepared according to a *Standard Procedure A* for the Sonogashira coupling reaction between iodo-nucleobase **C1** and the ethynyl-nucleobase **G1**. A dry a THF/NEt<sub>3</sub> (4:1) mixture (10 mL) was poured over, **G1<sub>alk2</sub><sup>[8b]</sup>** (60 mg 0.3 mmol), PdCl<sub>2</sub>(PPh<sub>3</sub>)<sub>2</sub> (4.1 mg, 6 μmol), and CuI (0.6 mg, 0.3 μmol). Then, **C1** (283 mg, 0.6 mmol), was added and the mixture was stirred under argon for 12h at 40 °C. Once completed, the mixture was filtrated over a celite plug and the solvent was evaporated under reduced pressure. The product was purified by recrystallization in acetonitrile, affording **GC0c** as an orange solid (123 mg, 75 %). <sup>1</sup>H NMR (300 MHz, [D<sub>6</sub>]DMSO, 25°C, TMS): δ= 10.90 (s (broad), 1H; NH<sup>16</sup>C), 8.26 (s, 1H; H<sup>6C</sup>), 7.96 (s (broad), 1H; NH<sup>4C</sup>), 7.26 (s (broad), 1H; NH<sup>4C</sup>), 6.82 (s (broad), 2H; NH<sub>2</sub><sup>2G</sup>), 5.79 (s, 1H; H<sup>1C</sup>), 5.03 (d, <sup>3</sup>J(H,H)=6.3 Hz, 1H; H<sup>2C</sup>), 4.82 (d, <sup>3</sup>J(H,H)=6.3 Hz, 1H; H<sup>2C</sup>), 4.26 (d, <sup>3</sup>J(H,H)=7.9 Hz, 3H; H<sup>4C</sup>, H<sup>5C</sup>), 4.07 (q, <sup>3</sup>J(H,H)=7.1, <sup>3</sup>J(H,H)=6.5 Hz, 2H; -CH<sub>2</sub>CH<sub>3</sub>), 2.64–2.52 (m, 1H; COCH), 1.48 (s, 3H; -OC(CH<sub>3</sub>)), 1.31 (d, <sup>3</sup>J(H,H)=7.3 Hz, 6H; -OC(CH<sub>3</sub>), -CH<sub>2</sub>CH<sub>3</sub>), 1.06 (dd, <sup>3</sup>J(H,H)=7.0, <sup>3</sup>J(H,H)=4.3 Hz, 6H; -COCH-(CH<sub>3</sub>)<sub>2</sub>). <sup>13</sup>C NMR (75 MHz, [D<sub>6</sub>]DMSO, 25°C, TMS): δ= 175.8, 164.0, 156.1, 154.4, 152.9, 150.8, 148.8, 129.4, 117.0, 112.9, 94.1, 88.4, 85.0, 84.4, 84.2, 83.7, 80.9, 64.0, 57.5, 57.5, 37.8, 33.1, 26.9, 25.1, 23.0, 19.2, 18.7, 18.6, 14.8, 13.4. HRMS (ESI+): *m/z* calcd for C<sub>25</sub>H<sub>31</sub>N<sub>8</sub>O<sub>7</sub>: 555.2316 [*M*+*H*]<sup>+</sup>; found: 555.2307 [*M*+*H*]<sup>+</sup>.

**GC0d** was prepared following *Standard Procedure A*. **G1<sub>Alk10</sub>** (0.15 g, 0.49 mmol), **C1<sub>Alk10</sub>** (0.18 g, 0.49 mmol), CuI (1.0 mg, 0.005 mmol) and Pd(PPh<sub>3</sub>)<sub>4</sub> (11.2 mg, 0.010 mmol) were suspended in the THF/NEt<sub>3</sub>

mixture (7 mL). The reaction was completed overnight. The resulting insoluble dark red solid in suspension was filtered and washed with THF and acetonitrile. **GC0d** was obtained as an ochre solid (77 mg, 28%). <sup>1</sup>H NMR (300 MHz, [D<sub>6</sub>]DMSO, 25°C, TMS): δ= 10.72 (s (broad), 1H; N<sup>16</sup>C), 8.41 (s, 1H; H<sup>6C</sup>), 8.14 (s (broad), 2H; C<sup>4C</sup>NH<sub>2</sub>), 7.66 (s (broad), 2H; C<sup>4C</sup>NH<sub>2</sub>), 6.62 (s (broad), 2H; C<sup>2G</sup>NH<sub>2</sub>), 4.04 (m, 2H; N<sup>8G</sup>CH<sub>2</sub>C<sub>9</sub>H<sub>19</sub>), 1.72 (s, 2H; N<sup>9G</sup>CH<sub>2</sub>CH<sub>2</sub>C<sub>8</sub>H<sub>17</sub>), 1.61 (s, 2H; N<sup>1C</sup>CH<sub>2</sub>CH<sub>2</sub>C<sub>8</sub>H<sub>17</sub>), 1.25–1.18 (m, 28H; N<sup>8G</sup>C<sub>2</sub>H<sub>4</sub>C<sub>7</sub>H<sub>14</sub>CH<sub>3</sub>, N<sup>1C</sup>C<sub>2</sub>H<sub>4</sub>C<sub>7</sub>H<sub>14</sub>CH<sub>3</sub>), 0.85–0.83 (m, 6H; N<sup>9G</sup>C<sub>9</sub>H<sub>18</sub>CH<sub>3</sub>, N<sup>1C</sup>C<sub>9</sub>H<sub>18</sub>CH<sub>3</sub>). <sup>13</sup>C NMR (75 MHz, [D<sub>6</sub>]DMSO, 25°C, TMS): δ= 159.1, 155.2, 154.9, 154.6, 145.7, 129.1, 109.4, 100.0, 95.0, 91.2, 87.4, 79.6, 52.1, 47.1, 46.2, 31.8, 31.7, 29.4, 29.34, 29.25, 29.2, 29.1, 28.9, 28.6, 26.2, 26.1, 22.6, 22.5, 13.89, 13.85, 8.4. HRMS (ESI+): *m/z* calcd for C<sub>31</sub>H<sub>49</sub>N<sub>8</sub>O<sub>2</sub> [*M*+*H*]<sup>+</sup>: 565.3972; found: 565.3989 [*M*+*H*]<sup>+</sup>.

**AU0** was prepared according to a *Standard Procedure A* for the Sonogashira coupling reaction between bromo-nucleobase **A<sub>alk10</sub><sup>[8b]</sup>** and the ethynyl-nucleobase **U1**. A dry a THF/NEt<sub>3</sub> (4:1) mixture (12 mL) was poured over **A<sub>alk10</sub><sup>[8b]</sup>** (50 mg 1.4 mmol), PdCl<sub>2</sub>(PPh<sub>3</sub>)<sub>2</sub> (1.9 mg, 3 μmol), and CuI (0.26 mg, 1.4 μmol). Then, **U1** (77 mg, 2 mmol), was added and the mixture was stirred under argon for 12h at 40 °C. Once completed, the mixture was filtrated over a celite plug and the solvent was evaporated under reduced pressure. The product was purified by column chromatography on silica gel eluted with CHCl<sub>3</sub>/MeOH (30:1), affording **AU0** as a white solid (48 mg, 51 %). <sup>1</sup>H NMR (300 MHz, [D<sub>6</sub>]DMSO, 25°C, TMS): δ= 11.90 (s (broad), 1H; NH<sup>3U</sup>), 8.26 (s, 1H; H<sup>6U</sup>), 6.86 (s (broad), 2H; NH<sup>2A</sup>), 5.99 (s (broad), 2H; NH<sup>2A</sup>), 5.83 (s, 1H; H<sup>1U</sup>), 5.11 (dd, <sup>3</sup>J(H,H)=7.0, <sup>3</sup>J(H,H)=4.3 Hz, 1H; H<sup>2U</sup>), 4.82 (dd, <sup>3</sup>J(H,H)=6.9, <sup>3</sup>J(H,H)=3.6 Hz, 1H; H<sup>3U</sup>), 4.33–4.02 (m, 5H; H<sup>4U</sup>, H<sup>5U</sup>, -NCH<sub>2</sub>-), 2.58 (m, 1H; -COCH), 1.50 (s, 3H; -OC(CH<sub>3</sub>)), 1.30 (s, 3H; -OC(CH<sub>3</sub>)), 1.24–1.06 (m, 16H; -CH<sub>2</sub>-), 1.08 (d, <sup>3</sup>J(H,H)=2.8 Hz, 3H; -COCH-(CH<sub>3</sub>)<sub>2</sub>), 1.06 (d, <sup>3</sup>J(H,H)=2.8 Hz, 3H; -COCH-(CH<sub>3</sub>)<sub>2</sub>), 0.83 (t, <sup>3</sup>J(H,H)=7.2 Hz, 3H; -CH<sub>2</sub>CH<sub>3</sub>). HRMS (ESI+): *m/z* calcd for C<sub>33</sub>H<sub>47</sub>N<sub>8</sub>O<sub>7</sub>: 667.3562 [*M*+*H*]<sup>+</sup>; found: 667.3584 [*M*+*H*]<sup>+</sup>.

**B'-HC** was prepared according to *Standard Procedure B* for the Sonogashira coupling reaction between the ethynyl-nucleobase **C1** and **B'-H**. A dry a THF/NEt<sub>3</sub> (4:1) mixture (10 mL) was poured over **B'-H** (537 mg, 1.32 mmol), PdCl<sub>2</sub>(PPh<sub>3</sub>)<sub>2</sub> (3.71 mg, 5.2 μmol), and CuI (0.5 mg, 2.65 μmol). Then, **C1** (100 mg, 0.27 mmol) was added dropwise and the mixture was stirred under argon for 12h at 40 °C. Once completed, the mixture was filtrated over a celite plug and the solvent was evaporated under reduced pressure. The product was purified by column chromatography on silica gel eluted with CHCl<sub>3</sub>/MeOH (20:1), affording **B'-HC** as a brown solid (120 mg, 67 %). The excess of **B'-H** was recovered. <sup>1</sup>H NMR (300 MHz, CDCl<sub>3</sub>, 25°C, TMS): δ= 8.07 (s (broad), 1H; NH<sup>4C</sup>), 7.76 (s, 1H; H<sup>6C</sup>), 7.70 (d, *J* = 8.2 Hz, 2H; *H*), 7.48 (s, 4H; H<sup>a,d</sup>), 7.28 (d, <sup>3</sup>J(H,H)=8.2 Hz, 2H; *H*<sup>b</sup>), 6.19 (s (broad), 1H; NH<sup>4C</sup>), 5.70 (s, 1H; H<sup>1C</sup>), 4.91 (d, <sup>3</sup>J(H,H)=6.5 Hz, 1H; H<sup>2C</sup>), 4.75 (t, <sup>3</sup>J(H,H)=5.1 Hz, 1H; H<sup>3C</sup>), 4.37–4.16 (m, 3H; H<sup>4C</sup>, H<sup>5C</sup>), 2.51 (hept, <sup>3</sup>J(H,H)=6.9 Hz, 1H; -COCH), 1.49 (s, 3H; -OC(CH<sub>3</sub>)), 1.27 (s, 3H; -OC(CH<sub>3</sub>)), 1.08 (2xd, <sup>3</sup>J(H,H)=7.0 Hz, 6H; -COCH-(CH<sub>3</sub>)<sub>2</sub>).

**GC'-H** was prepared between **B'-HC** and the ethynyl-nucleobase **G1**. A dry a THF/NEt<sub>3</sub> (4:1) mixture (12 mL) was poured over **B'-HC** (117 mg, 0.18 mmol), PdCl<sub>2</sub>(PPh<sub>3</sub>)<sub>2</sub> (2.5 mg, 3.6 μmol), and CuI (0.03 mg, 1.78 μmol). Then, **G1** (93 mg, 0.21 mmol), was added dropwise and the mixture was stirred under argon for 12h at 40 °C. Once completed, the mixture was filtrated over a celite plug and the solvent was evaporated under reduced pressure. The product was purified by recrystallization in methanol, affording **GC'-H** as a yellow solid (75 mg, 45 %). <sup>1</sup>H NMR (300 MHz, CDCl<sub>3</sub>: [D<sub>6</sub>]DMSO, 25°C, TMS): δ= 10.97 (s (broad), 1H; NH<sup>16</sup>C), 8.12 (s, 1H; H<sup>6C</sup>), 7.97 (s (broad), 1H; NH<sup>4C</sup>), 7.87 (d, <sup>3</sup>J(H,H)=8.3 Hz, 2H; *H*<sup>d</sup>), 7.82 (d, <sup>3</sup>J(H,H)=8.4 Hz, 2H; *H*), 7.73 (t, <sup>3</sup>J(H,H)=7.8 Hz, 4H; H<sup>a,e</sup>), 7.24 (s (broad), 1H; NH<sup>4C</sup>), 6.76 (s (broad), 2H; NH<sub>2</sub><sup>2G</sup>), 6.15 (s, 1H; H<sup>1G</sup>), 5.83 (s, 1H; H<sup>1C</sup>), 5.45 (d, <sup>3</sup>J(H,H)=6.2 Hz, 1H; H<sup>2G</sup>), 5.25 (dt, <sup>3</sup>J(H,H)=14.3, <sup>3</sup>J(H,H)=5.1 Hz, 1H; H<sup>2C</sup>), 5.02 (d, <sup>3</sup>J(H,H)=6.4 Hz, 1H; H<sup>3G</sup>), 4.84–4.81 (m, 1H; H<sup>3C</sup>), 4.32–4.14 (m, 6H; H<sup>4G</sup>, H<sup>5G</sup>, H<sup>4C</sup>, H<sup>5C</sup>), 2.57 (dd, <sup>3</sup>J(H,H)=14.2, <sup>3</sup>J(H,H)=7.2 Hz, 1H; -COCH), 1.52 (d, <sup>3</sup>J(H,H)=15.5 Hz, 6H;



-OC(CH<sub>3</sub>)<sub>2</sub>), 1.32 (d, <sup>3</sup>J(H,H)=13.3 Hz, 6H; -OC(CH<sub>3</sub>)<sub>2</sub>), 1.11 – 1.08 (m, 15H, -C(CH<sub>3</sub>)<sub>3</sub>; -COCH-(CH<sub>3</sub>)<sub>2</sub>). <sup>13</sup>C NMR (75 MHz, CDCl<sub>3</sub>:[D<sub>6</sub>]DMSO, 25°C, TMS): δ= 177.1, 175.8, 156.1, 154.6, 154.2, 150.3, 146.9, 140.3, 138.6, 132.3, 131.9, 127.1, 126.7, 122.1, 119.5, 117.5, 113.3, 113.0, 93.8, 93.1, 88.8, 85.4, 84.6, 84.4, 83.4, 81.5, 80.7, 79.6, 64.2, 63.9, 38.1, 33.1, 27.0, 26.9, 26.8, 25.3, 25.3, 25.1, 18.8, 18.7. HRMS (ESI+): *m/z* calcd for C<sub>50</sub>H<sub>55</sub>N<sub>8</sub>O<sub>12</sub>: 959.3939 [*M*+H]<sup>+</sup>; found: 959.3974 [*M*+H]<sup>+</sup>.

**B'-MeC** was prepared according to *Standard Procedure B* for the Sonogashira coupling reaction between the ethynyl-nucleobase **C1** and **B'-Me**. A dry a THF/NEt<sub>3</sub> (4:1) mixture (13 mL) was poured over **B'-Me** (322 mg, 0.7 mmol), PdCl<sub>2</sub>(PPh<sub>3</sub>)<sub>2</sub> (0.19 mg, 0.2 μmol), and CuI (0.02 mg, 0.13 μmol). Then, **C1** (52 mg, 13 μmol) was added dropwise and the mixture was stirred under argon for 12h at 40 °C. Once completed, the mixture was filtrated over a celite plug and the solvent was evaporated under reduced pressure. The product was purified by column chromatography on silica gel eluted with CHCl<sub>3</sub>/MeOH (20:1), affording **B'-MeC** as a brown solid (70 mg, 71 %). The excess of **B'-Me** was recovered. <sup>1</sup>H NMR (300 MHz, CDCl<sub>3</sub>, 25°C, TMS): δ= 8.90 (s (broad), 1H; NH<sup>H</sup>), 7.66 (s, 1H; H<sup>B</sup>), 7.43 (s, 2H; H<sup>I</sup>), 5.92 (s, 2H; H<sup>A</sup>), 5.67 (d, <sup>3</sup>J(H,H)=3.2 Hz, 1H; H<sup>I</sup>), 4.92 (d, <sup>3</sup>J(H,H)=6.2 Hz, 1H; H<sup>B</sup>), 4.74 (dd, <sup>3</sup>J(H,H)=6.3, <sup>3</sup>J(H,H)=3.6 Hz, 1H; H<sup>B</sup>), 4.44 – 4.18 (m, 3H; H<sup>A</sup>, H<sup>B</sup>), 2.53 (pd, <sup>3</sup>J(H,H)=7.0, <sup>3</sup>J(H,H)=2.1 Hz, 1H; -COCH), 1.91 – 1.73 (m, 12H; -CCH<sub>3</sub>), 1.50 (s, 3H; -OC(CH<sub>3</sub>)<sub>2</sub>), 1.28 (s, 3H; -OC(CH<sub>3</sub>)<sub>2</sub>), 1.09 (2xd, <sup>3</sup>J(H,H)=7.0 Hz, 6H; -COCH-(CH<sub>3</sub>)<sub>2</sub>).

**GC'-Me** was prepared between **B'-MeC** and the ethynyl-nucleobase **G1**. A dry a THF/NEt<sub>3</sub> (4:1) mixture (12 mL) was poured over **B'-MeC** (70 mg, 0.1 mmol), PdCl<sub>2</sub>(PPh<sub>3</sub>)<sub>2</sub> (1.4 mg, 2 μmol), and CuI (0.19 mg, 0.1 μmol). Then, **G1** (51 mg, 0.18 mmol), was added dropwise and the mixture was stirred under argon for 12h at 40 °C. Once completed, the mixture was filtrated over a celite plug and the solvent was evaporated under reduced pressure. The product was purified by recrystallization in methanol, affording **GC'-Me** as an orange solid (40 mg, 70 %). <sup>1</sup>H NMR (300 MHz, CDCl<sub>3</sub>:[D<sub>6</sub>]DMSO, 25°C, TMS): δ= 10.88 (s (broad), 1H; NH<sup>H</sup>), 8.0 (s, 1H; H<sup>B</sup>), 7.36 (d, <sup>3</sup>J(H,H)=13.8 Hz, 4H; H<sup>I</sup>), 6.96 (s (broad), 1H; NH<sup>H</sup>), 6.60 (s (broad), 2H; NH<sub>2</sub><sup>2G</sup>), 6.14 (s, 1H; H<sup>I</sup>), 5.82 (s, 1H; H<sup>I</sup>), 5.37 (d, <sup>3</sup>J(H,H)=6.2 Hz, 1H; H<sup>B</sup>), 5.29 – 5.25 (m, 1H; H<sup>B</sup>), 4.97 (d, <sup>3</sup>J(H,H)=6.3 Hz, 1H; H<sup>B</sup>), 4.80 (d, <sup>3</sup>J(H,H)=5.1 Hz, 1H; H<sup>B</sup>), 4.36 – 4.09 (m, 6H; H<sup>A</sup>, H<sup>B</sup>, H<sup>C</sup>), 2.61 – 2.53 (m, 1H; -COCH), 1.86 (d, <sup>3</sup>J(H,H)=6.2 Hz, 12H; -CH<sub>3</sub><sup>h,e</sup>), 1.54 (s, 3H; -OC(CH<sub>3</sub>)<sub>2</sub>), 1.49 (s, 3H; -OC(CH<sub>3</sub>)<sub>2</sub>), 1.33 (s, 3H; -OC(CH<sub>3</sub>)<sub>2</sub>), 1.29 (s, 3H; -OC(CH<sub>3</sub>)<sub>2</sub>), 1.10 – 1.07 (m, 15H; -C(CH<sub>3</sub>)<sub>3</sub>, -COCH-(CH<sub>3</sub>)<sub>2</sub>). <sup>13</sup>C NMR (75 MHz, CDCl<sub>3</sub>:[D<sub>6</sub>]DMSO, 25°C, TMS): δ= 177.1, 175.8, 164.1, 156.1, 154.1, 153.1, 150.3, 146.6, 141.0, 139.0, 136.0, 135.1, 130.7, 130.4, 129.0, 121.3, 119.0, 117.4, 113.3, 113.0, 94.0, 93.6, 93.3, 88.8, 85.4, 84.7, 84.4, 83.4, 81.5, 80.7, 78.2, 69.8, 64.2, 63.9, 38.1, 33.1, 27.0, 26.9, 26.8, 25.3, 25.1, 19.1, 18.7, 18.7. HRMS (MALDI; Matrix: DCTB): *m/z* calcd for C<sub>54</sub>H<sub>62</sub>N<sub>8</sub>NaO<sub>12</sub>: 1037.4385 [*M*+Na]<sup>+</sup>; found: 1037.4370 [*M*+Na]<sup>+</sup>.

## Acknowledgements

Funding from the European Research Council (ERC-StG 279548) and MINECO (CTQ2014-27729-P and CTQ2017-84727-P) is gratefully acknowledged (DGR). CFG gratefully acknowledges financial support from the Netherlands Organization for Scientific Research NWO (ECHO).

**Keywords:** Supramolecular Chemistry • Chelate Cooperativity • Conformational Effects

[1] O. J. G. M. Goor, S. I. S. Hendrikse, P. Y. W. Dankers, E. W. Meijer, *Chem. Soc. Rev.* **2017**, *46*, 6621.

- [2] P. Ballester, J. de Mendoza in *Modern Supramolecular Chemistry*, (Eds.: F. Diederich, P. J. Stang, R. R. Tykwinski), Wiley-VCH, Weinheim, **2008**, p. 69.
- [3] A. S. Mahadevi, G. N. Sastry, *Chem. Rev.* **2016**, *116*, 2775.
- [4] T. F. A. de Greef, M. M. J. Smulders, M. Wolfs, A. P. H. J. Schenning, R. P. Sijbesma, E. W. Meijer, *Chem. Rev.* **2009**, *109*, 5687.
- [5] M. J. Mayoral, N. Bilbao, D. González-Rodríguez, *ChemistryOpen* **2016**, *5*, 10.
- [6] G. M. Whitesides, E. E. Simanek, J. P. Mathias, C. T. Seto, D. N. Chin, M. Mammen, D. M. Gordon, *Acc. Chem. Res.* **1995**, *28*, 37.
- [7] J. D. Badjić, A. Nelson, S. J. Cantrill, W. B. Turnbull, J. F. Stoddart, *Acc. Chem. Res.* **2005**, *38*, 723.
- [8] a) C. A. Hunter, H. L. Anderson, *Angew. Chem. Int. Ed.* **2009**, *48*, 7488; b) G. Ercolani, L. Schiaffino, *Angew. Chem. Int. Ed.* **2011**, *50*, 1762; c) A. S. Mahadevi, G. N. Sastry, *Chem. Rev.* **2016**, *116*, 2775; d) L. K. S. von Krbek, C. A. Schalley, P. Thordarson, *Chem. Soc. Rev.* **2017**, *46*, 2622.
- [9] Focus Issue on Cooperativity, *Nat. Chem. Biol.* **2008**, *4*, 433.
- [10] a) F. Würthner, C.-C. You, C. R. Saha-Möller, *Chem. Soc. Rev.* **2004**, *33*, 133; b) M. Fujita, M. Tominaga, A. Hori, B. Therrien, *Acc. Chem. Res.* **2005**, *38*, 371; c) R. Chakrabarty, P. S. Mukherjee, P. J. Stang, *Chem. Rev.* **2011**, *111*, 6810; d) T. R. Cook, P. J. Stang, *Chem. Rev.* **2015**, *115*, 7001.
- [11] T. K. Ronson, S. Zarra, S. P. Black, J. R. Nitschke, *Chem. Commun.* **2013**, *49*, 2476.
- [12] G. Guichard, I. Huc, *Chem. Commun.* **2011**, *47*, 5933.
- [13] a) H. J. Hogben, J. K. Sprafke, M. Hoffmann, M. Pawlicki, H. L. Anderson, *J. Am. Chem. Soc.* **2011**, *133*, 20962; b) J. K. Sprafke, B. Odell, T. D. W. Claridge, H. L. Anderson, *Angew. Chem. Int. Ed.* **2011**, *50*, 5572.
- [14] a) G. Ercolani, *Struct. Bond.* **2006**, *121*, 167; b) H. Sun, C. A. Hunter, C. Navarro, S. Turega, *J. Am. Chem. Soc.* **2013**, *135*, 13129; c) S. Di Stefano, G. Ercolani in *Advances in Physical Organic Chemistry*, (Eds.: I. H. Williams, N. H.; Williams), Elsevier Ltd., **2016**, Vol. 50, Chapter 1, pp. 1; d) P. Motloch, C. A. Hunter, C. A. in *Advances in Physical Organic Chemistry*, (Eds.: I. H. Williams, N. H.; Williams), Elsevier Ltd., **2016**, Chapter 2, Vol. 50, pp. 77.
- [15] a) C. Montoro-García, J. Camacho-García, A. M. López-Pérez, N. Bilbao, S. Romero-Pérez, M. J. Mayoral, D. González-Rodríguez, *Angew. Chem. Int. Ed.* **2015**, *54*, 6780; b) S. Romero-Pérez, J. Camacho-García, C. Montoro-García, A. M. López-Pérez, A. Sanz, M. J. Mayoral, D. González-Rodríguez, *Org. Lett.* **2015**, *17*, 2664; c) C. Montoro-García, J. Camacho-García, A. M. López-Pérez, M. J. Mayoral, N. Bilbao, D. González-Rodríguez, *Angew. Chem. Int. Ed.* **2016**, *55*, 223; d) C. Montoro-García, M. J. Mayoral, R. Chamorro, D. González-Rodríguez, *Angew. Chem. Int. Ed.* **2017**, *56*, 15649.
- [16] a) J. Camacho-García, C. Montoro-García, A. M. López-Pérez, N. Bilbao, S. Romero-Pérez, D. González-Rodríguez, *Org. Biomol. Chem.* **2015**, *13*, 4506; b) N. Bilbao, V. Vázquez-González, M. T. Aranda, D. González-Rodríguez, *Eur. J. Org. Chem.*, **2015**, *54*, 7160.
- [17] Other authors have been synthesized similar G-C derivatives by click chemistry, see for example: a) T. Bhattacharyya, P. Saha, J. Dash, *ACS Omega*, **2018**, *3*, 2230; b) R. N. Das, Y. P. Kumar, S. A. Kumar, O. M. Schütte, C. Steinem, J. Dash, *Chem. Eur. J.*, **2018**, *24*, 4002; c) R. N. Das, Y. P. Kumar, O. M. Schütte, C. Steinem, J. Dash, *J. Am. Chem. Soc.*, **2015**, *137*, 34; d) Y. P. Kumar, R. N. Das, S. Kumar, O. M. Schütte, C. Steinem, J. Dash, *Chem. Eur. J.* **2014**, *20*, 3023.
- [18] a) C. Fonseca Guerra, H. Zijlstra, G. Paragi, F. M. Bickelhaupt, *Chem. Eur. J.* **2011**, *17*, 12612; b) A. Likhitsup, R. J. Deeth, S. Otto, A. Marsh, *Org. Biomol. Chem.*, **2009**, *7*, 2093.
- [19] X. Du, J. Zhou, J. Shi, B. Xu, *Chem. Rev.*, **2015**, *115*, 13165.
- [20] a) G. te Velde, F. M. Bickelhaupt, E. J. Baerends, C. Fonseca Guerra, S. J. A. van Gisbergen, J. G. Snijders, T. Ziegler, *J. Comput. Chem.* **2001**, *22*, 931; b) ADF2017, SCM, Theoretical Chemistry, Vrije Universiteit Amsterdam, The Netherlands, <http://www.scm.com>.
- [21] a) I. Ceccelli, G. Prampolini, *J. Phys. Chem. A*, **2003**, *107*, 8665; b) E. Masson, *Org. Biomol. Chem.* **2013**, *11*, 2859.
- [22] N. Bilbao, I. Destoop, S. De Feyter, D. González-Rodríguez, *Angew. Chem. Int. Ed.* **2016**, *55*, 659.

---

[23] D. Vonlanthen, J. Rotzler, M. Neuburger, M. Mayor, *Eur. J. Org. Chem.* **2010**, 120.

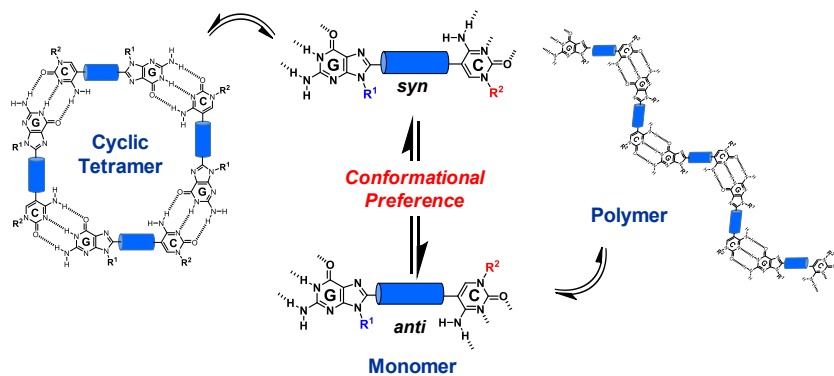
---

---

## Entry for the Table of Contents

## FULL PAPER

---



*Carlos Montoro-García, Nerea Bilbao,  
Iris M. Tsagri, Francesco Zaccaria, Maria  
J. Mayoral, Célia Fonseca Guerra\* and  
David González-Rodríguez\**

**Page No. – Page No.**

**Impact of Conformational Effects on  
the Ring-Chain Equilibrium of  
Hydrogen-bonded Dinucleosides**

**Supramolecular ring vs chain** equilibria in complementary dinucleoside monomers is here dominated by subtle factors ruling the equilibrium between different conformations that orient Watson-Crick H-bonding interfaces.

---